International Journal of Engineering Research and Development
e- ISSN: 2278-067X, p-ISSN: 2278-800X, www.ijerd.com
Volume 22, Issue 6 (June 2026), PP 138-145

Single crystals of Mn^{2+} doped $LuPO_4$ with optical absorption and local structure

Maroj Bharati [1], Vikram Singh [2], Ram Kripal [3]
[1] Department of Physics, Nehru Gram Bharti (DU), Jamunipur, Prayagraj-221505,Uttar Pradesh, India
[2] Department of Physics, Nehru Gram Bharti (DU), Jamunipur, Prayagraj-221505,Uttar Pradesh, India
[3] EPR Laboratory, Department of Physics, University of Allahabad, Prayagraj-211002, Uttar Pradesh, India
***Corresponding Author**: Ram Kripal*

Abstract
The zero field splitting parameters for the Mn^{2+} doped crystals of $LuPO_4$ are estimated from the superposition model. The obtained parameters are in good agreement with the experimental ones. The experimental conclusion that the Mn^{2+} ion replaces the Lu^{3+} site in $LuPO_4$ is supported by theoretical investigation. Using the crystal field parameters derived from the superposition model and the crystal field analysis program, the optical spectra of the crystal are computed by diagonalizing the total Hamiltonian. There is a reasonable match between the calculated and experimental band positions. Thus, the theoretical analysis validates the experimental observations.

Keywords: *Inorganic compounds, Electron paramagnetic resonance, Zero field splitting, Single crystal, Crystal fields, Superposition model.*

Date of Submission: 05-06-2026 Date of acceptance: 16-06-2026

I. Introduction

EPR is a powerful tool of spectroscopy for studying the solid state chemistry of crystals as the EPR spectrum can identify the impurity and its valence state as well as provide the local crystalline electric-field symmetry of the paramagnetic ion [1]. Since Mn^{2+} produces EPR lines even at room temperature, it is the most researched transition metal ion. It has a $^6S_{5/2}$ ground state and a $3d^5$ electronic configuration. Zero field splitting of Mn^{2+} in crystals is very sensitive to small structural changes in the crystal [2-6].

The zero field splitting (ZFS) and crystal field (CF) parameters can be modeled taking the superposition model (SPM) for application in EPR [7-9] and optical spectroscopy [10-11]. The spin Hamiltonian (SH) in addition to other Hamiltonians is discussed in [12]. The crystal field (CF) parameters are often obtained using SPM and the point-charge model [13] while there is exchange charge model (ECM) as well for analyzing the effects of crystal fields in single crystals doped with rare earth and transition metal ions [14]. In this study, SPM is employed to calculate the ZFS parameters and the CF parameters. SPM was suggested for CF based on certain assumptions [15]. Obtaining a static polar coordinate system (R_L, θ_L, ΦL) for each ligand or ion from the host crystal's X-ray data is crucial for performing an SPM analysis on the CF. Ionic size, ionic charge, and inter-ionic bonding mismatches will likely cause some local distortion when transition metal ions are added. Critical analysis of experimental spin-Hamiltonian parameters for Mn^{2+} and Fe^{3+} in CaO and MgO crystals has been performed [16]. It provides the precise values of the SPM parameters and shows that the CF for 3d ions satisfies the superposition principle. For the alkali earth oxides, sets of SPM intrinsic parameters based on reliable ligand distances were determined using a rigorous lattice relaxation model [17].

$LuPO_4$ crystallizes in the zircon structure, which is shared by rare-earth vanadates and arsenates, as well as the natural minerals zircon ($ZrSiO_4$) and xenotime (RPO_4, R = Y, Tb to Lu, and Sc). Plutonic igneous rocks also contain zircon variants with actinide or transition-metal ion impurities occupying the Zr sites. The use of zircon and rare-earth orthophosphates as a nuclear waste storage medium has been investigated due to their high melting temperatures, structural and chemical stability, resistance to radiation damage, and long-term corrosion resistance. Understanding the thermodynamic behavior of these materials under the temperature-pressure and radiation-damage conditions that are common in the earth requires knowledge of the phonon properties. Zircon-type crystalline hosts, in general, exhibit good optical quality (refractive index of 1.8–2.0, birefringence of 0.04–0.10), and phonons play a vital role in the luminescence properties of transition-metal-doped crystals [18]. For example, the charge-transfer-type luminescence of Yb^{3+} and Sb^{3+} ions in RPO_4 (R = Sc, Lu, and Y) indicates vibronic coupling involving phonons of energies of about 270 ±30 cm^{-1} [19]. The cooperative Jahn-Teller phase transitions in several stoichiometric rare-earth phosphates and vanadates, which involve coupling of the rare-earth crystal-field-split states with acoustic or low-lying optic phonons, have been investigated by Raman scattering and infrared absorption [20, 21].

Recently, several synthetic analogues of natural minerals have been assessed for their potential application as stable chemical hosts to isolate high-level radioactive nuclear wastes from the biosphere permanently. In particular, the favorable long-term geological stability of the natural orthophosphate minerals xenotime and monazite ($LnPO_4$ with Ln = La, Ce, Pr, ...) has prompted a series of investigations of the properties of analogous synthetic rare-earth orthophosphates which could chemically incorporate high-level nuclear wastes [22, 23]. In recent years, single crystals and powders of rare-earth orthophosphate systems both with, and without, the addition of simulated nuclear waste have been prepared and characterized using a variety of methods [24-29]. EPR spectroscopy [28] has proven to be particularly useful in these characterizations, since many of the elements comprising the nuclear waste material are present in the orthophosphate (and other) hosts with valence states such that unpaired electrons are present. The technique can also be applied to investigations of impurities in nuclear waste glasses and polycrystalline ceramics [30]. An opportunity to learn more about the solubility, site symmetry, and other solid state chemical characteristics of an aliovalent ion is presented by investigating manganese as a divalent impurity in lanthanide orthophosphates. One significant class of high-level nuclear waste contains manganese. Accordingly, divalent manganese incorporated as a dilute impurity in both single crystals and powders of the zircon-structure host, $LuPO_4$ has been investigated [31]. Mn^{2+}-doped $LuPO_4$ is characterized by its high density; luminescent properties induced by Mn^{2+}, good thermal stability, and potentially altered magnetic properties. These properties make it a promising material for various applications, including phosphors, solid-state lasers, and other optical and electronic devices. Charge compensating mechanisms that can be local and lessen the crystal field symmetry from the orthophosphate host's tetragonal symmetry are required when the divalent Mn^{2+} ion is introduced into substitutional Lu^{3+} metal sites. The introduction of the divalent Mn^{2+} ion into substitutional Lu^{3+} metal sites needs charge compensating mechanisms that can be local and reduce the crystal field symmetry from the orthophosphate host's tetragonal symmetry. Mn^{2+} ion is observed to occupy the magnetically inequivalent orthorhombic sites in $LuPO_4$ single crystal. The spin Hamiltonian parameters at room temperature have been reported [31].

Using CF parameters derived from SPM and perturbation equations, the ZFS parameters D and E are determined for the Mn^{2+} ion in $LuPO_4$ at the substitutional Lu^{3+} site at 293 K (room temperature, RT) in this investigation [32]. The goal is to locate the Mn2+ ion and the distortion occurring within the crystal. Reasonable agreement is found between the experimental values and the results obtained for the Mn^{2+} ion at the substitutional Lu^{3+} site in the $LuPO_4$ crystal with local distortion. In order to build an SPM parameter database, the study also aims to determine the degree to which Mn^{2+} ions in $LuPO_4$ crystals can be subjected to CF theory and SPM analysis. This will estimate the design of molecular nano magnets (MNMs) and computer modeling of their spectroscopic and magnetic properties. The transition ion-based MNM class currently includes single-molecule magnets (SMM) [33], single-chain magnets (SCM) [34], and single ion magnets (SIM) [35]. The intriguing magnetic properties of MNM, such as magnetization's macroscopic quantum tunneling and possible uses in high-density information storage and quantum computing, have attracted a lot of attention from researchers to the aforementioned systems [33, 34]. Mn^{2+} and Cr^{3+} ions are present in a number of synthetic SCM or SMM systems [36]. Since model calculations for simpler systems can be used as a basis for more complex ones, the parameters of the model developed in this study may be used for ZFS parameter calculations for Mn^{2+} ions at comparable sites in MNM. Crystals of scientific and industrial significance in a number of other ion-host systems can be investigated using the modeling carried out in this work.

2. Crystal Structure

Lutetium phosphate, or $LuPO_4$, crystallizes as a tetragonal zircon-type structure and belongs to the space group $I4_1/amd$ (D_{4h}^{19}, No. 141). The tetragonal lattice has the parameters a =6.792, b = 6.792, c = 5.954 Å, Z =4 [37]. The metal atom has two distinct metal-oxygen bond distances and is eight-coordinated to oxygen atoms. Each of these discrete lengths is tetrahedrally oriented orthogonal to the others forming the dodecahedron. The dodecahedron is a distorted cube that can be visualized to give its point group by viewing it as two perpendicular trapezoids. Furthermore, two interpenetrating tetrahedra can be found in a cube that has been distorted to reduce repulsions between oxygen atoms while preserving a favorable metal-oxygen interaction. The resulting eight-vertice polyhedron made up of the two interpenetrating bisphenoids is commonly referred to as a bisbisphenoid (symmetry D_{2d}), and the distorted tetrahedra are known as bisphenoids (symmetry D_{2d}). The dodecahedron's eight vertices are separated into two sets of bisphenoids, but they are not equivalent. Figure 1 shows the symmetry adopted axis system (SAAS) and crystal structure of $LuPO_4$.

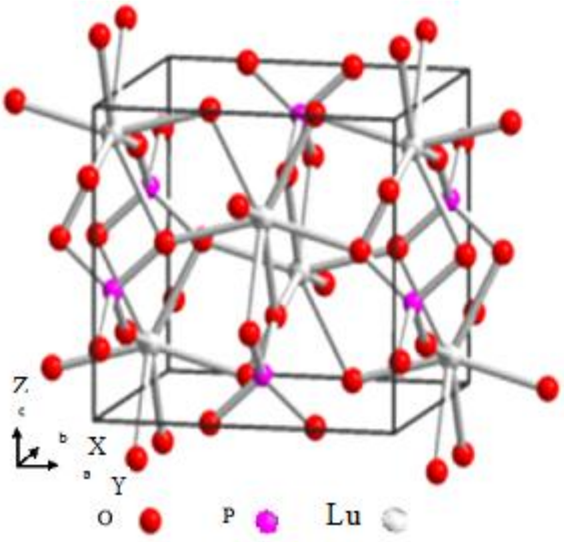

Fig. 1. The crystal structure of $LuPO_4$ at room-temperature and the symmetry-adopted axis system (SAAS).

II. Calculations of Crystal Field and Zero Field Splitting Parameters

The below spin Hamiltonian is used to analyze EPR spectra [8]:

$$\mu_B B.g.S + D\left\{S_Z^2 - \frac{1}{3}S(S+1)\right\} + E(S_x^2 - S_y^2) = \mathcal{H} \qquad (1)$$

The applied magnetic field, Bohr magneton, spectroscopic splitting factor, second rank axial, and second rank rhombic ZFS parameters are represented by the letters B, μB, g, D, and E [38–39]. The a, b, and c crystal axes along with the laboratory axes (x, y, z) are shown in Fig. 1. The mutually perpendicular directions of metal-ligand bonds are referred to as the local symmetry axes or the symmetry adopted axes (SAA) of the site. As displayed in Fig.1, the axis-Z of SAAS is along the crystal axis- c, and (X, Y) are perpendicular to the axis-Z. In the $LuPO_4$ crystal, doped Mn^{2+} ions enter the lattice at substitutional Lu^{3+} sites with a certain amount of local distortion [40].

The spin Hamiltonian for a $3d^5$ ion is written as [41],

$$\mathcal{H} = \mathcal{H}_o + \mathcal{H}_{so} + \mathcal{H}_{ss} + \mathcal{H}_C \qquad (2)$$

$$\mathcal{H}_C = \sum B_{kq} C_q^{(k)} \qquad (3)$$

where B_{kq} (in Wybourne notation) are the CF parameters and $C_q^{(k)}$ are the spherical tensor operators. $B_{kq} \neq 0$ in the crystal field of orthorhombic symmetry only for k = 2, 4; q = 0, 2, 4. The CF parameters B_{kq} are calculated using SPM [42].

The symmetry of the local field about Mn^{2+} ions in the $LuPO_4$ crystal is considered to be orthorhombic (OR-type I) [8]. In this symmetry, the ZFS parameters D and E are obtained as follows [42]:

$$D = \left(\frac{3\varsigma^2}{70P^2D'}\right)[-B_{20}^2 - 21\varsigma B_{20} + 2B_{22}^2] + \left(\frac{\varsigma^2}{63P^2G}\right)[-5B_{40}^2 - 4B_{42}^2 + 14B_{44}^2]$$

(4)

$$E = \left(\frac{\sqrt{6}\varsigma^2}{70P^2D'}\right)[2B_{20} - 21\varsigma]B_{22} + \left(\frac{\varsigma^2}{63P^2G}\right)[3\sqrt{10}B_{40} + 2\sqrt{7}B_{44}]B_{42}$$

(5)

Here P = 7B+7C, G = 10B+5C, D' = 17B+5C. B and C represent Racah parameters and ς is the spin-orbit coupling parameter. Considering average covalency parameter N, $B = N^4B_0$, $C = N^4 C_0$, $\varsigma = N^2\varsigma_0$, where ς_0 is free ion spin-orbit coupling parameter and B_0 and C_0 are free ion Racah parameters [41, 43]. The free Mn^{2+} ion has $B_0 = 960$ cm^{-1}, $C_0 = 3325$ cm^{-1} and $\varsigma_0 = 336$ cm^{-1} [8].

The parameter N is found from N = ($\sqrt{B/B_0} + \sqrt{C/C_0}$)/2 taking Racah parameters (B = 917 cm^{-1}, C = 2254 cm^{-1}) obtained from optical analysis of Mn^{2+} ion in zinc ammonium phosphate hexahydrate, the crystal having oxygen ligands [44], since there is no reporting of optical study of Mn^{2+} doped $LuPO_4$ in literature.

The CF parameters, in terms of co-ordination factor $K_{kq}(\theta_j, \varphi_j)$ and intrinsic parameter $\overline{A_k}(R_j)$, using SPM are obtained [15, 42] as

$$B_{kq} = \sum_j \overline{A_k}(R_j) K_{kq}(\theta_j, \phi_j) \tag{6}$$

$\overline{A_k}(R_j)$ is written as

$$\overline{A_k}(R_0)\left(\frac{R_0}{R_j}\right)^{t_k} = \bar{A}_k(R_j) \tag{7}$$

where the ligand's distance from the d^n ion is denoted by R_j, $\overline{A_k}(R_0)$ is the intrinsic parameter, R_0 is the reference distance from the metal ion to the ligand and t_k gives power law exponent. For crystals doped with Mn^{2+} ion, $t_2 = 3$ and $t_4 = 7$ are taken [42]. Since the Mn^{2+} ion's coordination is octahedral, $\overline{A_4}$ is estimated from the relation [45]

$$\overline{A_4}(R_0) = \frac{3}{4} Dq \tag{8}$$

From optical study [44], $Dq = 756$ cm^{-1}. Therefore, $\overline{A_4}(R_0) = 567$ cm^{-1}. For $3d^5$ ions the ratio $\frac{\overline{A_2}}{\overline{A_4}}$ lies in the range 8 - 12 [41, 46-47]. With $\frac{\overline{A_2}}{\overline{A_4}} = 10$, $\overline{A_2} = 5670$ cm^{-1}.

III. Results and Discussion

Utilising SPM, parameters $\overline{A_2}$ and $\overline{A_4}$, and the ligand arrangement about Mn^{2+} ion as indicated in Fig. 1, the CF parameters of the Mn^{2+} ion at the substitutional Lu^{3+} sites are evaluated. Atomic coordinates in $LuPO_4$ single crystal, bond length R (with and without distortion), and angles θ, φ for site I are provided in Table 1. The CF parameters and ZFS parameters together with reference distance R_0 are given in Table 2. Table 2 shows that ZFS parameters for substitutional octahedral site I differ from the experimental values [31] with $R_0 = 0.200$ nm being slightly smaller than the sum of ion radii (0.223 nm) of $Mn^{2+} = 0.083$ nm and $O^{2-} = 0.140$ nm and no distortion. Experimental ZFS parameter values |D| and |E| for site I are 177.3×10^{-4} cm^{-1}, 8.3×10^{-4} cm^{-1}, respectively. |E|/|D| is found as 0.047 being smaller than the standard value 0.333 [39]. |D| and |E| determined theoretically without distortion are larger than the experimental values. The value of |E|/|D| is also larger than the standard value 0.333 [39]. As a result, the computation takes local distortion into account. The ZFS parameters for substitutional octahedral site I are in good agreement with the experiment's values, with the R_0 value and local distortion above [31]. ZFS parameters close to experimental values have been calculated using the parameters $t_2 = 3$ and $t_4 = 7$ with transformation S2 for standardization [39] to get |E|/|D| ratio < 0.333.

Table 1. Atomic coordinates, bond length R (both with and without distortion), and angles θ, φ in $LuPO_4$ single crystal (site I).

Location of Mn^{2+}	Ligands	x	y (Å)	z	R(nm)	θ^0	φ^o
					Spherical polar co-ordinates of ligands		
			Without distortion				
Site : Substitutional Lu	O1	0.0000	0.4262	0.2126	0.2260 R_1	87.77 θ_1	90.00 φ_1
(0.0000, 0.7500,	O2	0.0000	-0.4262	0.2126	0.8005 R_2	89.37 θ_2	90.00 φ_2
0.1250)	O3	0.0000	0.9262	0.0374	0.1305 R_3	93.84 θ_3	90.00 φ_3
	O4	0.0000	0.0738	0.0374	0.4622 R_4	91.08 θ_4	90.00 φ_4
	O5	- 0 .4262	0.0000	-0.2126	0.6194 R_5	93.12 θ_5	93.95 φ_5
	O6	0.4262	0.5000	0.4626	0.3912 R_6	85.05 θ_6	83.72 φ_6
			With distortion				
I	O1				0.5560	72.77	91.50
	O2				0.9905	99.37	92.00
	O3				0.2705	105.84	92.00
	O4				0.6072	90.58	96.00
	O5				0.8044	108.12	93.95
	O6				0.4762	70.05	85.72

Table 2. The crystal field and zero field splitting parameters of the Mn^{2+} doped $LuPO_4$ crystal.

		Crystal- field parameters (cm^{-1})					Zero-field splitting parameters ($10^{-4}cm^{-1}$)		
Site	R_0(nm)	B_{20}	B_{22}	B_{40}	B_{42}	B_{44}	|D|	|E |	|E|/|D|
			Without distortion						
Site I $\frac{\bar{A}_2}{\bar{A}_4}=10$	0.200	-25498.8	-31461.5	32906.84	35007.44	47583.73	33303.3	14524.4	0.436
			With distortion						
Site I $\frac{\bar{A}_2}{\bar{A}_4}=10$	0.200	-3139.84	1965.327	66.2917	97.21412	2242.043	177.3	47.8	0.269
						Exp.	177.3	8.3	0.047

The optical spectra of Mn^{2+} doped $LuPO_4$ single crystals are computed using the CFA program [48] and B_{kq} parameters (with distortion). The locations of the Mn^{2+} ion's energy bands are established following the diagonalization of the total Hamiltonian.

The energy band locations for substitutional site I are displayed in Table 3 according to calculation and experimental data [44].

Table 3. The positions of energy bands of single crystal of $LuPO_4$ doped Mn^{2+}, both calculated and experimental.

Transition from $^6A_{1g}(S)$	Observed band (cm^{-1})	Calculated band (cm^{-1}) I

$^4T_{1g}(G)$	16044	20430, 20435, 21251, 21268, 21364, 21389
$^4T_{2g}(G)$	20433	21672, 21680, 21782, 21807, 21843, 21874
$^4E_g(G)$	24108	22382, 22402, 22646, 22663
$^4A_{1g}(G)$	24242	23547, 23563
$^4T_{2g}(D)$	26724	26743, 26814, 26904, 26969, 27302, 27330
$^4E_g(D)$	30451	30239, 30417, 30528, 30589
$^4T_{1g}(P)$	33956	32787, 32816, 32883, 32994, 33404, 33476
$^4A_{2g}(F)$	36846	36866, 36925
$^4T_{1g}(F)$	38521	37563, 37649, 37709, 37765, 39635, 39639

The calculated and experimental energy band positions agree quite well, as Table 3 demonstrates. Thus, the experimental discovery [31, 44] that Mn^{2+} ions enter the $LuPO_4$ crystal at the substitutional octahedral site is supported by the theoretical results. Table 3 shows a good agreement between calculated and experimental energy band positions. Therefore, the theoretical results support the experimental finding [31, 44] that Mn^{2+} ions enter the $LuPO_4$ crystal at the substitutional octahedral site.

IV. Conclusions

Zero field splitting parameters using perturbation theory and the superposition model for $LuPO_4$ single crystals doped with Mn^{2+} ions are obtained. The ZFS parameters calculated agree well with the experimental values. The calculated positions of the optical energy bands match reasonably well with those obtained from the experiment. Therefore, the theoretical analysis that Mn^{2+} ions occupy substitutional sites in $LuPO_4$ supports the experimental result. ZFS parameter determinations for Mn^{2+} ions at similar locations in molecular nano magnets may be performed using the model parameters derived from this investigation. Crystals with a wide range of scientific and industrial uses can be found using the current modeling technique.

Acknowledgement

The authors express their gratitude to Prof. C. Rudowicz of the Faculty of Chemistry at Adam Mickiewicz University in Poznan, Poland, for the CFA program, and to the Head of the Physics Department at Allahabad University in Allahabad for providing the department's facilities.

Declarations

Ethical Approval:

There were no human or animal subjects in this study, and it wasn't conducted in any protected or private locations. Corresponding locations did not require any special permissions.

Conflicting interests:

The authors affirm that no known conflicting financial interests or personal relationships could have influenced any of the work presented in this paper.

Authors' contributions:

Vikram Singh and Maroj Bharati prepared the figure, wrote the manuscript, and carried out the computations.
Ram Kripal: concept and oversight.
The manuscript has been reviewed by all authors.

Funding:
There is no funding received..

Availability of data and materials:
Upon request, the data will be made available.

References

[1]. J. A. Weil, J. R. Bolton, Electron Paramagnetic Resonance: Elementary Theory and Practical Applications; 2nd ed., Wiley, New York, 2007.

[2]. L. A. Boatner, M. M. Abraham, and M. Rappaz, Scientific Basis/or Nuclear Waste Management, edited by J. G. Moore, Vol. 3, p. 181, Plenum, New York, 1981).

[3]. F. E. Mabbs, D. Collison, D. Gatteschi, Electron Paramagnetic Resonance of d Transition Metal Compounds; Elsevier, Amsterdam, 1992.

[4]. R. M. Krishna, V. P. Seth, S. K. Gupta, D. Prakash, I. Chand, J. L. Rao, EPR of Mn^{2+}-ion-doped single crystals of $Mg[C_4H_3O_4]_2\cdot 6H_2O$, Spectrochim. Acta A **53** (1997) 253-258.

[5]. D. Halder, Y. Jana, D. Piwowarska, P. Gnutek, C. Rudowicz, Tailoring single-ion magnet properties of coordination polymer $C_{11}H_{18}DyN_3O_9$ (Dy-CP) using the radial effective charge model (RECM) and superposition model (SPM), Phys. Chem. Chem. Phys.26(2024) 19947-19959.

[6]. S. P. Rathee, S. S. Hooda, EPR and superposition-model analysis of zero-field splitting parameters for Mn2+ doped in ZnNbOF5.6H2O and CoNbOF5.6H2O single crystals, Indian J. Phys. 99(1)(2025)145-148.

[7]. C. Rudowicz, P. Gnutek, M. Açıkg¨oz, Superposition model in electron magnetic resonance spectroscopy – a primer for experimentalists with illustrative applications and literature database, Appl. Spectrosc. Rev. 54 (2019) 673–718.

[8]. A. Abragam, B. Bleaney, Electron Paramagnetic Resonance of Transition Ion, Dover, New York, 1986.

[9]. J. R. Pilbrow, Transition-Ion Electron Paramagnetic Resonance, Clarendon Press, Oxford, 1990.

[10]. B. G. Wybourne, Spectroscopic Properties of Rare Earth, Wiley, New York, 1965.

[11]. J. Mulak, Z. Gajek, The Effective Crystal Field Potential, Elsevier, Amsterdam, 2000.

[12]. R. Boˇca, Zero-field splitting in metal complexes, Coord. Chem. Rev. 248 (2004) 757–815.

[13]. M. G. Brik, N. M. Avram (Eds.). Optical Properties of 3d-Ions in Crystals: Spectroscopy and Crystal Field Analysis. Heidelberg: Springer, (2013), Y. Y. Yeung: Chapter 3, pp. 95-121.

[14]. [M. G. Brik, N. M. Avram, C. N. Avram, Crystal Field Analysis of Cr^{3+} Energy Levels in $LiGa_5O_8$ Spinel, Acta Phys. Polon. A112 (2007) 1055-1060.

[15]. D. J. Newman and B. Ng, The superposition model of crystal fields, Rep. Prog. Phys. 52 (1989) 699-763.

[16]. D. J. Newman, E. Siegel**,** Superposition model analysis of Fe^{3+} and Mn^{2+} spin-Hamiltonian parameters, J. Phys. C: Solid State Phys. 9 (1976) 4285-4292.

[17]. Y. Y. Yeung, Local distortion and zero-field splittings of $3d^5$ ions in oxide crystals, J. Phys. C: Solid State Phys. 21 (1988)2453-2462.

[18]. J. O. Nriagu, P. B. Moore, and F. Betts, Phosphate Minerals, Springer-Verlag, Berlin, 1984.

[19]. E. W. J. L. Oomen, W. M. A. Smit, and G. Blasse, Jahn-Teller effect in the emission and excitation spectra of the Sb^{3+} ion in LPO_4 (L = Sc, Ln, Y), Phys. Rev. B **37** (1988)18-26.

[20]. R. T. Harley, in Spectroscopy of Solids Containing Rare Earth Ions, edited by A. Kapyanskii and R. M. Macfarlane, Elsevier, Amsterdam, 1987, p. 557.

[21]. G. A. Gehring and K. A. Gehring, Co-operative Jahn-Teller effects, **Rep. Prog. Phys. 38 (1975) 1-90.**

[22]. L. A. Boatner, G. W. Beall, M. M. Abraham, C. B. Finch, P. G. Huray, and M. Rappaz, Scientific Basis/or Nuclear Waste Management, edited by C. J. Northrup, Vol. 2, p. 289, Plenum, New York, 1980.

[23]. L. A. Boatner, G. W. Beall, M. M. Abraham, C. B. Finch, R. J. Floran, P. G. Huray, and M. Rappaz, Management of Alpha-Contaminated Wastes, IAEA-SM-246/73, p. 411, I.A.B.A., Vienna, 1981.

[24]. W. O. Milligan, D. F. Mullica, G. W. Beall, and L. A. Boatner, The structures of three lanthanide orthophosphates, Inorg. Chim. Acta 70 (1983) 133-136.

[25]. M. Begun, G. W. Beall, L. A. Boatner, and W. T. Gregor, Raman spectra of the rare earth orthophosphates, J. Raman Spectrosc. 11 (1981) 273-278.

[26]. P. C. Becker, N. Edelstein, G. M. Williams, J. J. Bucher, R. E. Russo, J. O. Koningstein, L. A. Boatner, and M. M. Abraham, Intensities and asymmetries of electronic Raman scattering in $ErPO_4$ and $TmPO_4$, Phys. Rev. B 31 (1985) 8102-8110.

[27]. M. M. Abraham, L. A. Boatner, J. O. Ramey, and M. Rappaz, An EPR study of rare-earth impurities in single crystals of the zircon-structure orthophosphates $ScPO_4$, YPO_4, and $LuPO_4$, J. Chem. Phys. 78 (1983) 3-10.

[28]. M. Rappaz, J. O. Ramey, L. A. Boatner, and M. M. Abraham, EPR investigations of Fe^{3+} in single crystals and powders of the zircon-structure orthophosphates $LuPO_4$, YPO_4, and $ScPO_4$**,** J. Chem. Phys. 76 (1982)40-45.

[29]. B. C. Sales, C. W. White, and L. A. Boatner, A comparison of the corrosion characteristics of synthetic monazite and borosilicate glass containing simulated nuclear defense waste, Nucl. Chem. Waste Manage.4 (1983) 281-289.

[30]. M. Rappaz, M. M. Abraham, and L. A. Boatner, Alternate Nuclear Waste Forms and Interactions in Geologic Media, USDOE, CONF-8005107, edited by L. A. Boatner and G. C. Battle, Jr., U.S. GPO, Washington, D.C., 1981.

[31]. J. L. Boldú O., E. Muñoz P., M. M. Abraham, and L. A. Boatner, EPR and thermoluminescence investigations of Mn^{2+} in $LuPO_4$, YPO_4, and $ScPO_4$, J. Chem. Phys.83(1985)6113-6120.

[32]. W. L. Yu, M.G. Zhao, Spin-Hamiltonian parameters of ^6S state ions. Phys. Rev. B 37(1988) 9254-9267.

[33]. G. Aromí, E. K. Brechin, Synthesis of 3d metallic single-molecule magnets, Struct. Bonding 122 (2006) 1-67.

[34]. C. Coulon, H. Misayaka, R. Clérac, Single-Chain Magnets: Theoretical Approach and Experimental Systems, Struct. Bonding 122 (2006) 163-206.

[35]. M. Murrie, Cobalt(II) single-molecule magnets, Chem. Soc. Rev. 39 (2010) 1986-1995.

[36]. C. van Wüllen, Magnetic anisotropy through cooperativity in multinuclear transition metal complexes: theoretical investigation of an anisotropic exchange mechanism, Mol. Phys. 111 (2013) 2392–2397.

[37]. W. O. Milligan, D. F. Mullica, G. W. Beall, L. A. Boatner, Structural Investigations of YPO_4, $ScPO_4$, and $LuPO_4$, Inorg. Chim. Acta 60(1982)39-43.

[38]. C. J. Radnell, J. R. Pilbrow, S. Subramanian, M. T. Rogers, Electron paramagnetic resonance of Fe^{3+} ions in $(NH_4)_2SbF_5$. J. Chem. Phys. 62(1975) 4948-4952.

[39]. C. Rudowicz, R. Bramley, On standardization of the spin Hamiltonian and the ligand field Hamiltonian for orthorhombic symmetry. J. Chem. Phys. 83(1985) 5192- 5197.

[40]. B. N. Figgis, M. A. Hitchman, Ligand Field Theory and its Applications; Wiley, New York, 2000.

[41]. T. H. Yeom, S. H. Choh, M. L. Du, M. S. Jang, EPR study of Fe^{3+} impurities in crystalline $BiVO_4$. Phys. Rev. B 53(1996) 3415-3421.

[42]. T. H. Yeom, S. H. Choh, M. L. Du, A theoretical investigation of the zero-field splitting parameters for an Mn^{2+} centre in a $BiVO_4$ single crystal. J. Phys.: Condens. Matter 5(1993) 2017-2024.

[43]. C. K. Jorgensen, Modern Aspects of Ligand Field Theory; North- Holland, Amsterdam, 1971, p.305.

[44]. R. Kripal, H. Govind, S. K. Gupta, M. Arora, EPR and optical absorption study of Mn^{2+}-doped zinc ammonium phosphate hexahydrate single crystals, Physica B 392 (2007) 92-98.

[45]. D. J. Newman, B. Ng (Eds.), Crystal Field Handbook; Cambridge University Press, Cambridge, 2000.

[46]. A. Edgar, Electron paramagnetic resonance studies of divalent cobalt ions in some chloride salts. J. Phys. C: Solid State Phys. 9(1976) 4303-4314.

[47]. R. Kripal, M. G. Misra, A. K. Yadav, P. Gnutek, M. Açıkgöz, C. Rudowicz, Theoretical Analysis of Crystal field Parameters and Zero field Splitting Parameters for Mn^{2+} ions in Tetramethylammonium Tetrachlorozincate, Polyhedron, 235(2023)116341.

[48]. Y. Y. Yeung, C. Rudowicz, Crystal Field Energy Levels and State Vectors for the $3d^N$ Ions at Orthorhombic or Higher Symmetry Sites. J. Comput. Phys. 109(1993) 150-152.